# Particle dynamics in TOI-178 planetary system

Jovan Boskovic<sup>1,4</sup>, Rafael Sfair<sup>2,1,3\*</sup>, Christoph M. Schäfer<sup>1</sup>

<sup>1</sup>Institute for Astronomy and Astrophysics, Department of Computational Physics, University of Tübingen, Auf der Morgenstelle 10, 72076 Tübingen, Germany.

<sup>2</sup>UNESP - São Paulo State University, Av. Ariberto Pereira da Cunha, 333, Guaratinguetá, 12516-410, São Paulo, Brazil.

<sup>3</sup>LIRA, Observatoire de Paris, Université PSL, Sorbonne Université, Université Paris Cité, CY Cergy Paris Université, CNRS, 5 Place Jules Janssen, Meudon, 92190, Île-de-France, France.

<sup>4</sup>Institute of Aerodynamics and Gas Dynamics, University of Stuttgart, Wankelstraße 3, 70563 Stuttgart, Germany.

\*Corresponding author(s). E-mail(s): rafael.sfair@unesp.br; Contributing authors: jovan.boskovic@iag.uni-stuttgart.de; ch.schaefer@uni-tuebingen.de;

### Abstract

The TOI-178 system hosts six planets with five of them locked in a 2:4:6:9:12 Laplace resonance chain. We perform N-body simulations to investigate the dynamics of test particles in this system. We observe that co-orbital regions around each planet are approximately 30% wider than predicted by classical theory for planets in the resonance chain, while TOI-178b, which lies outside the chain, shows a 52% enhancement. The region between TOI-178e and TOI-178f reveals Kirkwood gap-like structures created by mean-motion resonances with TOI-178f (4:3, 5:4, 6:5) and TOI-178g (5:3), where particle clearing occurs on 500-year timescales. An extended integration of the innermost region (0.015-0.025 au) shows periodic inclination oscillations with period 196 years, coincident with TOI-178b's own oscillation period, with maximum amplitude occurring near the 3:2 resonance location. These structures are consistent with the system's resonant architecture and provide a baseline characterization that enables future comparative studies of similar phenomena in other multi-planet systems with resonant configurations.

Keywords: exoplanetary systems, N-body simulations, resonances, co-orbital regions

# 1 Introduction

The discovery and characterization of multi-planetary systems have provided insights into planetary formation and evolution processes. Among these systems, those exhibiting mean-motion resonances (MMRs) are particularly valuable, as they preserve information about their formation history [1–4]. Resonant configurations are generally considered fragile, meaning that significant scattering events or giant impacts would likely disrupt the resonant chain [5–7]. Thus, systems with resonant architectures serve as pristine laboratories for studying the outcome of protoplanetary discs.

Multi-planet systems in resonant chains represent a small but significant fraction of known exoplanetary systems [3, 8], with notable examples including TRAPPIST-1 [9, 10], Kepler-90 [11], K2-138 [12], Kepler-223 [1], and HD 110067 [13]. The dynamics of small bodies in such systems have received increasing attention, with studies revealing complex structures analogous to those observed in our Solar System [14–16].

The TOI-178 system, discovered through TESS observations and confirmed with follow-up observations from CHEOPS, ESPRESSO, NGTS, and SPECULOOS, represents a remarkable example of such resonant architecture [5]. This system consists of six transiting planets orbiting a V = 11.95 mag K-dwarf star. The planets range from super-Earth to mini-Neptune in size, with radii between 1.1–2.9  $R_{\oplus}$  and orbital periods of 1.91, 3.24, 6.56, 9.96, 15.23, and 20.71 days [5, 17, 18]. The five outer planets form a 2:4:6:9:12 chain of Laplace resonances, while the innermost planet lies just outside the resonant chain [5].

A particularly intriguing feature of TOI-178 is the non-monotonic variation in planetary densities across the system. Unlike other known resonant systems where density typically decreases with distance from the star, TOI-178 shows significant variations in density between adjacent planets [5, 18]. For instance, planet d has a significantly lower density than its inner neighbor c, despite being closer to the star than planet e, which has a higher density [5]. These density variations present challenges to standard formation and evolution models.

Recent work by Leleu et al. [18] has refined the planetary parameters through combined photodynamical modeling and radial velocity measurements, confirming that the system is indeed locked in a resonant configuration with the three Laplace angles librating around equilibrium values. The orbital structure of TOI-178 is extremely sensitive to perturbations, with Leleu, A. et al. [5] demonstrating that changing any planetary period by just  $\sim 0.01$  days could result in a chaotic system.

While the orbital architecture and physical properties of the TOI-178 planets have been extensively studied, the dynamics of test particles in this complex resonant system remains unexplored. Similar investigations for other systems, such as TRAPPIST-1, have revealed rich dynamical structures including stable and unstable regions shaped by resonances [19–21]. Studies of debris dynamics in the Solar System have demonstrated how planetary resonances create Kirkwood gap structures. [22–24], providing a framework for understanding similar phenomena in exoplanetary systems.

In this work, we investigate the dynamics of test particles in the TOI-178 system using N-body simulations. We aim to characterize the system's dynamical architecture, identify stable and unstable regions, examine the formation of resonance-induced

structures analogous to Kirkwood gaps in our Solar System, and investigate the stability of co-orbital regions. This baseline characterization provides a foundation for understanding small body dynamics in this multi-planet resonant chain and enables future comparative studies with other exoplanetary architectures.

The remainder of this paper is organized as follows. In Section 2, we describe our numerical simulation setup, including the planetary parameters, integration methods, and initial conditions for the test particles. Section 3 presents the results of our simulations, focusing on the global distribution of particles, co-orbital region widths, resonance-induced gaps, and inclination dynamics. Finally, in Section 4, we summarize our findings and discuss the implications of our results.

# 2 Numerical simulations

We investigated particle dynamics in the TOI-178 system using N-body simulations with the REBOUND package [25]. Calculations were performed using the IAS15 integrator [26], which employs adaptive time-stepping to maintain precision while preserving energy properties comparable to symplectic integrators. We used the default error tolerance of IAS15 ( $\sim 10^{-9}$ ) to ensure adequate precision for the close encounters and collision detection in our simulations.

Throughout this work, we use the terms "test particle" and "particle" equivalently to refer to massless objects that serve as dynamical probes of the gravitational environment. These particles do not gravitationally influence the planetary system but respond to the combined gravitational field of the star and planets, allowing us to map the system's dynamical structures.

Our simulations incorporated the six known planets of the TOI-178 system, with orbital elements and physical parameters adopted from [5] as summarized in Table 1. The central star was modeled with a mass of  $0.650~\rm M_{\odot}$ . Each planet was assigned a physical radius equal to 10% of its Hill radius for collision detection purposes. We adjusted the planetary inclinations to establish a reference plane where TOI-178c has an inclination of 0°, with all other inclinations measured relative to this plane. Note that Table 1 shows the original inclinations from [5] relative to the sky plane; in our simulations, these values are adjusted such that TOI-178c serves as the reference.

The orbital elements were computed for the reference epoch BJD 2458741.0 following [5]. Initial mean longitudes were calculated from TESS observations according to

$$\lambda_P = -\left(\frac{2\pi}{P_P}\right) \left(T_{0,P} - \text{date}_{ci}\right) - \frac{\pi}{2} \tag{1}$$

where  $\lambda_P$  is the mean longitude of planet P at the reference epoch dateci,  $P_P$  is the orbital period of planet P, and T0, P is the mid-transit time of planet P from [5]. The quantity dateci represents the first observation day in BJD-TBD, with  $P_P$  and  $(T0, P-\text{date}_{ci})$  expressed in consistent time units. The negative sign accounts for backward time propagation from the transit epoch to the reference epoch, while the  $-\pi/2$  term represents the orbital phase at which transit occurs (when the planet crosses

the observer's line of sight). For all planets, the other orbital elements (argument of pericentre  $\omega$ , longitude of ascending node  $\Omega$ , and mean anomaly M) were set to zero.

 ${\bf Table~1}~{\bf Orbital~elements~and~physical~parameters~of~the~TOI-178~planets.}$ 

Parameter	TOI-178b	TOI-178c	TOI-178d	TOI-178e	TOI-178f	TOI-178g
a [au]	0.02607	0.0370	0.0592	0.0783	0.1039	0.1275
e	0.0035	0.0119	0.0080	0.0080	0.0105	0.0056
$i [\deg]$	88.8	88.4	88.58	88.71	88.723	88.823
$M [\mathrm{M}_{\oplus}]$	1.50	4.77	3.01	3.86	7.72	3.94
$R\left[\mathrm{R}_{\oplus}\right]$	1.152	1.669	2.572	2.207	2.287	2.87
P [days]	1.91	3.24	6.56	9.96	15.23	20.71

In our primary simulation, we distributed  $10^6$  test particles using a random uniform distribution in semi-major axis (0.02 to 0.13 au) and mean anomaly (0 to  $2\pi$ ). All test particles were initialized with circular orbits (eccentricity = 0) and the same inclination as TOI-178c (inclination =  $0^{\circ}$  in our reference frame). Particles were removed from the simulation upon collision with any planet (approaching within the planet's physical radius) or when escaping the system (semi-major axis exceeding 0.3 au, approximately twice the distance of TOI-178g from the star).

We integrated the system for 500 years, with orbital parameters recorded at 10,000 equally spaced time points. We also conducted two additional targeted simulations to examine specific regions of interest. The first placed 10,000 test particles between 0.08 and 0.1 au (between TOI-178e and TOI-178f) and integrated for 500 years. The second focused on the innermost region (0.015-0.025 au) with 10,000 particles and extended to 10,000 years to analyze longer-term dynamical effects. Both simulations maintained the same planetary configurations and collision/escape criteria as the main simulation.

While these integration timescales are insufficient for full secular evolution (requiring  $\sim 10^8$  orbital periods), they are appropriate for the dynamical phenomena investigated here. Co-orbital clearing occurs on planetary clearing timescales, which can be estimated using the criterion presented in Eq.3 below, with the most massive planet TOI-178f requiring approximately 17,500 years to clear its neighboring regions. Kirkwood gap formation develops within hundreds of years, and inclination oscillations complete multiple cycles within our timeframe. Our 500-year integration corresponds to approximately 8,818 orbital periods of the outermost planet TOI-178g (P = 20.71 days), providing sufficient temporal coverage to capture the relevant clearing and resonant phenomena. Longer integrations with the current particle count ( $10^6$ ) would be computationally prohibitive for this exploratory study.

### 3 Results

Our numerical simulations of test particle dynamics in the TOI-178 system reveal distinct structures shaped by the multi-resonant planetary configuration. We first examine the global distribution of particles after 500 years, followed by quantitative

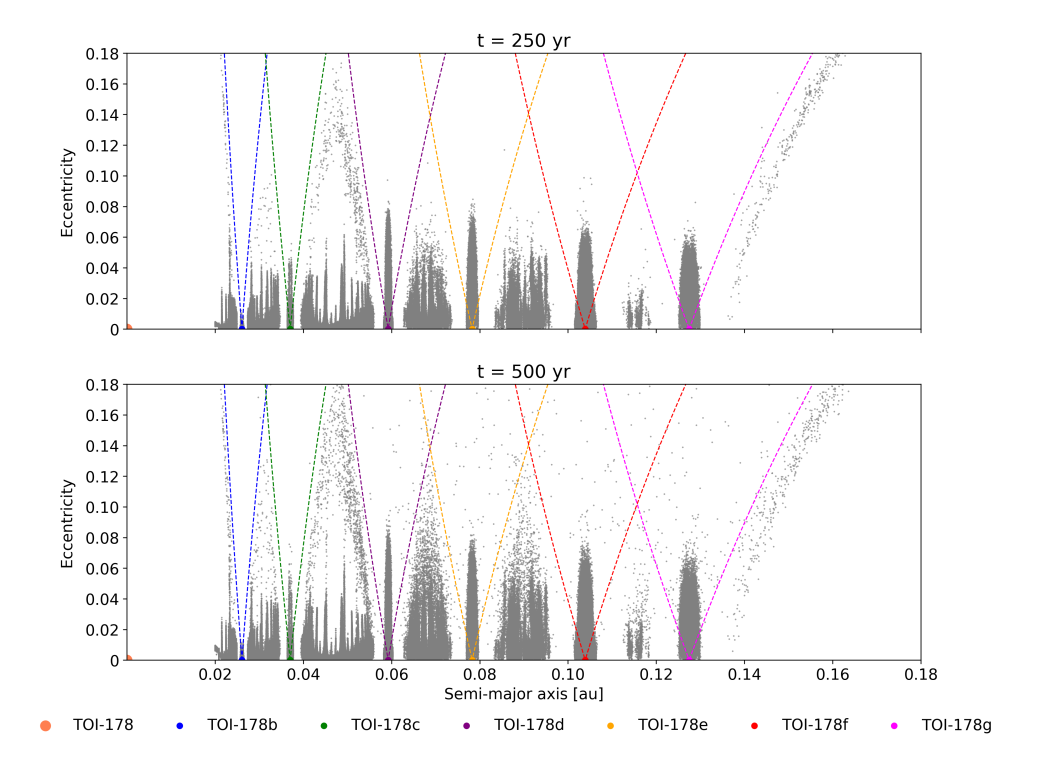


Fig. 1 Eccentricity versus semi-major axis distribution of test particles after 250 years (top panel) and 500 years (bottom panel), corresponding to approximately 4409 orbits and 8818 orbits for TOI-178g. Colored points mark planets, solid point at origin indicates TOI-178. Colored dotted lines indicate orbits matching perihelion and aphelion to specific planets semi-major axes (in the same color).

analysis of co-orbital regions and their deviation from theoretical predictions. We then present evidence for resonance-induced gaps between TOI-178e and TOI-178f, and conclude with an investigation of inclination oscillations in the inner disk region near TOI-178b.

### 3.1 Particle dynamics and resonant structures

Our numerical simulations of test particle dynamics in the TOI-178 system reveal distinct structural patterns shaped by the multi-resonant planetary architecture. The gravitational influence of the six planets creates a complex landscape of stable and unstable regions, with characteristic features associated with mean-motion resonances.

Figure 1 shows the eccentricity versus semi-major axis distribution after 500 years. The grey points represent test particles that survived the integration period, forming distinctive structural patterns throughout the system. Each planet in the TOI-178 system is represented by a colored point, with the central star shown in red at the origin. The dashed dotted curves indicate boundaries where particle perihelion (left) or aphelion (right) equals the semi-major axis of each planet.

The surviving particles predominantly occupy a confined region with semi-major axes between 0.02 au and 0.13 au and eccentricities below 0.1. Clear vertical bands in particle density are visible throughout this region, particularly near the planetary orbits and at key resonance locations. These bands represent zones where resonant perturbations have either stabilized or destabilized particle orbits, creating a complex structure of enhanced and depleted particle densities. The particles accumulate primarily between planetary orbits, with their distribution bounded by perihelion and aphelion constraints that prevent close encounters with the planets.

The dynamical evolution of particles during planetary encounters is governed by the Tisserand relation, given by

$$\frac{1}{2a}\sqrt{a(1-e^2)}\cos I = \frac{1}{2a'}\sqrt{a'(1-e'^2)}\cos I',\tag{2}$$

where primed variables denote post-encounter values. This relation, which approximates a conserved quantity in the restricted three-body problem, explains the characteristic boundaries in the (a, e) distribution, particularly evident beneath the aphelion line of TOI-178g at the right edge of the figure.

The efficiency with which planets clear their orbital neighborhoods depends on their mass and orbital separation. Following Margot [27], the clearing timescale can be quantified as

$$t_{\text{clear}} = C^2 \, 1.1 \times 10^5 \, \text{yr} \left( \frac{M_{\text{star}}}{M_{\odot}} \right)^{5/6} \left( \frac{M_p}{M_{\oplus}} \right)^{-4/3} \left( \frac{a}{1 \, \text{au}} \right)^{3/2},$$
 (3)

where  $C=2\sqrt{3}$  is a dimensionless constant related to the width of the cleared zone. The clearing timescales for the TOI-178 system range from  $\sim$ 5800 years for TOI-178c to  $\sim$  30,000 years for TOI-178g. For context, an Earth-like planet orbiting a Sun-like star at 1 au clears a region of  $\approx 3R_{H,\oplus}$  of test particles in approximately  $10^6$  years.

The test particle distribution exhibits a rich resonant structure, with pronounced vertical features at mean-motion resonances throughout the system. Figure 2 presents a histogram analysis of the particle distribution with 1000 bins from 0.02 au to 0.13 au, revealing clear gaps near planetary orbits and co-orbital regions. Notable features include persistent high-eccentricity populations at the 3:2 resonance of TOI-178d ( $\sim$ 0.045 au) and the 2:1 resonance of TOI-178f ( $\sim$ 0.065 au). Of particular interest are the Kirkwood gap-like structures in the region between TOI-178e and TOI-178f, visible in Figure 1 as vertical striations at approximately 0.085 au, 0.09 au, and 0.095 au, corresponding to specific resonances with the outer planets.

### 3.2 Co-orbital region widths

The particle distribution analysis reveals distinct co-orbital zones surrounding each planet in the TOI-178 system. These regions, characterized by significant particle

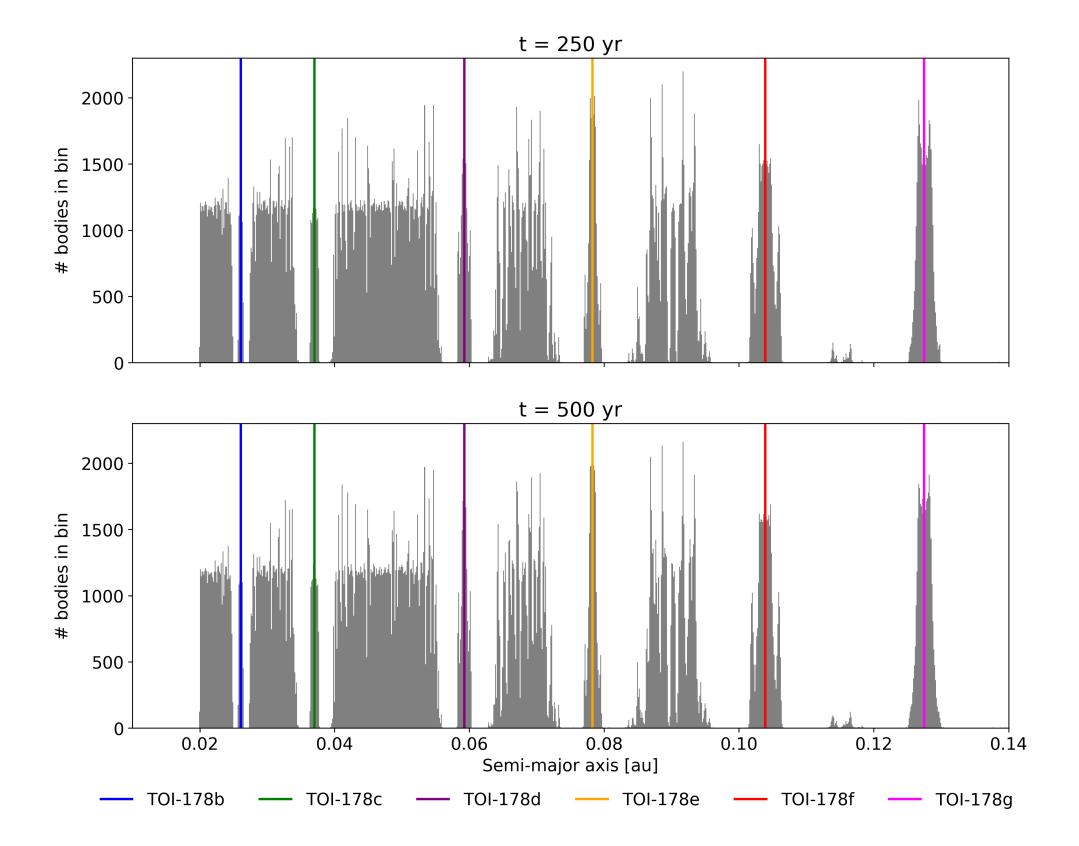


Fig. 2 Particle distribution (number of bodies in bins of size  $1.3 \times 10^{-4}$  au) evolution at 250 (top panel) and 500 years (bottom panel), corresponding to approximately 4409 orbits and 8818 orbits for TOI-178g. Planetary semi-major axes are indicated by solid lines.

depletion, represent domains where the gravitational influence of each planet effectively clears its orbital neighborhood. To quantify the extent of these clearing zones, we employ a threshold-based methodology for measuring co-orbital widths.

Given our initial distribution of  $10^6$  test particles, we establish a minimum threshold of 20 particles (approximately 1.5% of typical peak values) to define the boundaries of each co-orbital zone. This approach allows for precise determination of the cleared regions despite the statistical noise inherent in numerical simulations. Table 2 presents a comprehensive comparison between the measured co-orbital widths and theoretical predictions based on Dermott and Murray [28], whose analytical model gives:

$$W_{\rm hs} \sim 0.5 \mu a_{\rm sat}$$
 (4)

where  $W_{\rm hs}$  represents half the horseshoe width,  $a_{\rm sat}$  denotes the satellite's semi-major axis, and  $\mu$  is the mass ratio between the planet and the central star. This classical

formula provides a first-order approximation for co-orbital zone widths in the circular restricted three-body problem.

**Table 2** Comparison of co-orbital region size: theory vs simulation (in  $[\times 10^{-3} \text{ au}]$ ).

Planet	$W_{hs, { m theo}}$	$W_{hs, sim}$	Relative difference (% of $W_{hs, sim}$ )
TOI-178b	0.497	1.04	52.21
TOI-178c	1.037	1.56	33.51
TOI-178d	1.424	2.21	35.58
TOI-178e	2.046	2.86	28.47
TOI-178f	3.421	5.07	32.54
TOI-178g	3.377	4.94	31.64

Our results reveal significant and systematic deviations from the theoretical predictions. Planets within the resonance chain (TOI-178c through TOI-178g) exhibit co-orbital regions approximately 30% larger than predicted by the Dermott and Murray [28] model, with remarkably consistent relative differences ranging from 28.47% to 35.58%. We hypothesize that this enhancement may be related to the complex gravitational architecture of the resonance chain. Supporting this hypothesis, planets within the chain show remarkably consistent enhancement factors (28-36%), while the non-chain planet TOI-178b exhibits a distinctly larger enhancement (52%). This systematic difference suggests that different mechanisms may govern co-orbital dynamics in chain versus non-chain planets, though direct causal evidence requires further investigation through controlled simulations with varied resonant configurations.

The most pronounced deviation occurs for TOI-178b, which shows a 52.21% enhancement in its co-orbital width compared to theoretical predictions. This substantial increase is particularly noteworthy as TOI-178b remains outside the resonant chain that links the other planets. The enhanced clearing suggests that the standard prefactor of 0.5 in the Dermott and Murray [28] formula might underestimate the true co-orbital extent for non-chain planets in compact multi-planetary systems.

These systematic deviations highlight the limitations of simplified analytical models when applied to complex resonant architectures like TOI-178. The consistency of enhancement factors within the resonance chain suggests that multi-planet resonant interactions may create more extensive clearing zones than predicted by two-body models, though this hypothesis requires systematic testing through future simulations with varied resonant configurations.

# 3.3 Kirkwood gap-like structures between TOI-178e and TOI-178f

The region between TOI-178e and TOI-178f provides a detailed investigation of gap formation in a confirmed multi-planet Laplace resonance chain. Unlike the Solar System's asteroid belt, where gaps primarily result from Jupiter's isolated gravitational influence [29], the TOI-178 system presents a case where multiple planets in the

2:4:6:9:12 resonance chain simultaneously perturb particles through overlapping meanmotion resonances. This configuration allows us to examine how resonant planetary architectures shape small body distributions.

Analysis of this region reveals structures analogous to the Kirkwood gaps but with characteristics specific to multi-planet resonant systems. The structures develop through simultaneous resonant interactions with both TOI-178f and TOI-178g, creating zones of depleted particle density at overlapping mean-motion resonances - a phenomenon not observable in single-planet dominated environments like our Solar System's main belt [23].

To investigate these structures in detail, we conducted a focused simulation with 10,000 test particles distributed between 0.08-0.1 au and tracked their evolution over 500 years. Figure 3 shows the formation of prominent gaps at specific resonances: 0.089 au (5:4 resonance with TOI-178f), 0.091 au (5:3 resonance with TOI-178g), and 0.092 au (6:5 resonance with TOI-178f). Additional gaps of similar depth are visible at approximately 0.088 au, though the specific resonant origin of this feature requires further investigation. We note that these gaps are not precisely centered at the nominal resonance locations, with typical offsets of 0.001-0.002 au from theoretical predictions, consistent with the finite libration widths and eccentricity effects in the actual system. A broader gap appears at 0.086 au, corresponding to the 4:3 resonance with TOI-178f. The 5:3 resonance with TOI-178g creates gaps in a region where TOI-178f's resonances alone would not predict significant clearing, suggesting the enhanced dynamical complexity introduced by the resonance chain architecture. These locations align with mean-motion resonances where particles experience strong perturbations that eventually clear them from their orbits.

The resonance-driven clearing mechanism can be quantified using the libration width formula from resonance theory. Following [30], the maximum width of a resonance in semi-major axis is given by

$$\frac{\delta a_{max}}{a} = \pm \sqrt{\left(\frac{16|C_r|}{3n}e\right)\left(1 + \frac{|C_r|}{27j_2^2e^3n}\right)} - \frac{2|C_r|}{9j_2en},\tag{5}$$

where  $\delta a_{max}$  represents the maximum libration width, a is the semi-major axis at the exact resonance location,  $C_r$  denotes the resonance coefficient derived from the disturbing function, n is the mean motion of the particle, e is the orbital eccentricity, and  $j_2$  is the coefficient of the mean longitude in the resonance argument.

Figure 4 demonstrates particle depletion within these theoretical libration zones. Red regions represent resonances with TOI-178f, while the magenta region shows the 5:3 resonance with TOI-178g. Comparing the state at 100 and 500 years reveals systematic clearing of resonant zones, with particles accumulating along the boundaries. The 5:4 and 5:3 resonances exhibit particularly rapid clearing, with substantial depletion occurring within the first 100 years of evolution. This rapid timescale (hundreds of years) may be influenced by the coherent gravitational perturbations from multiple planets in the resonance chain, as opposed to the longer clearing timescales typically associated with isolated planet-particle interactions [31].

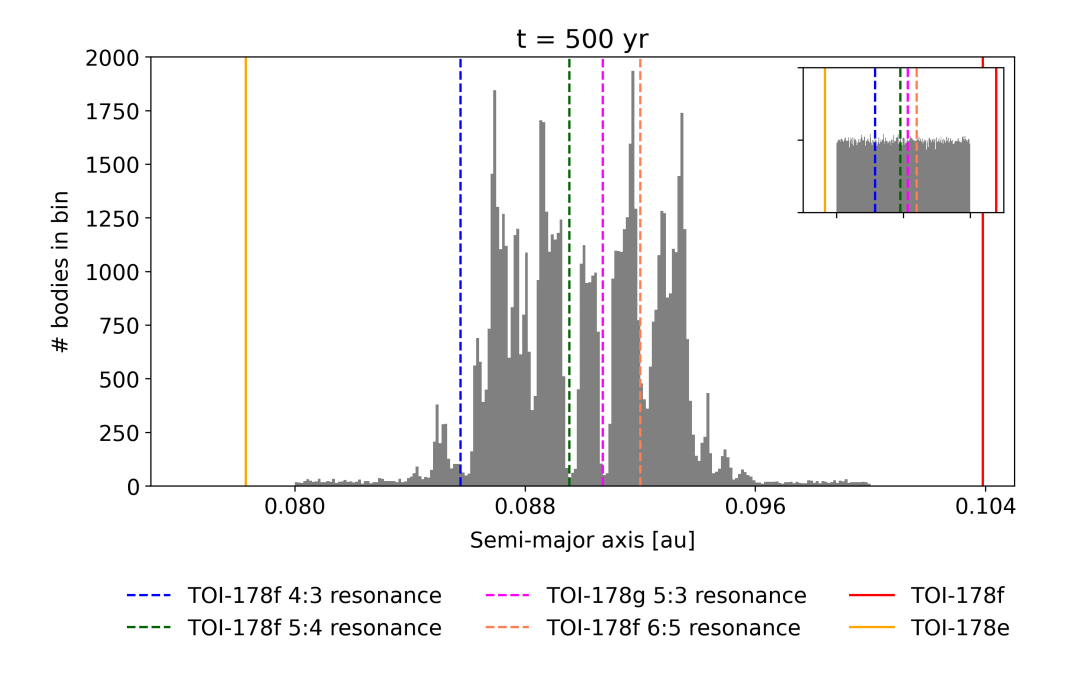
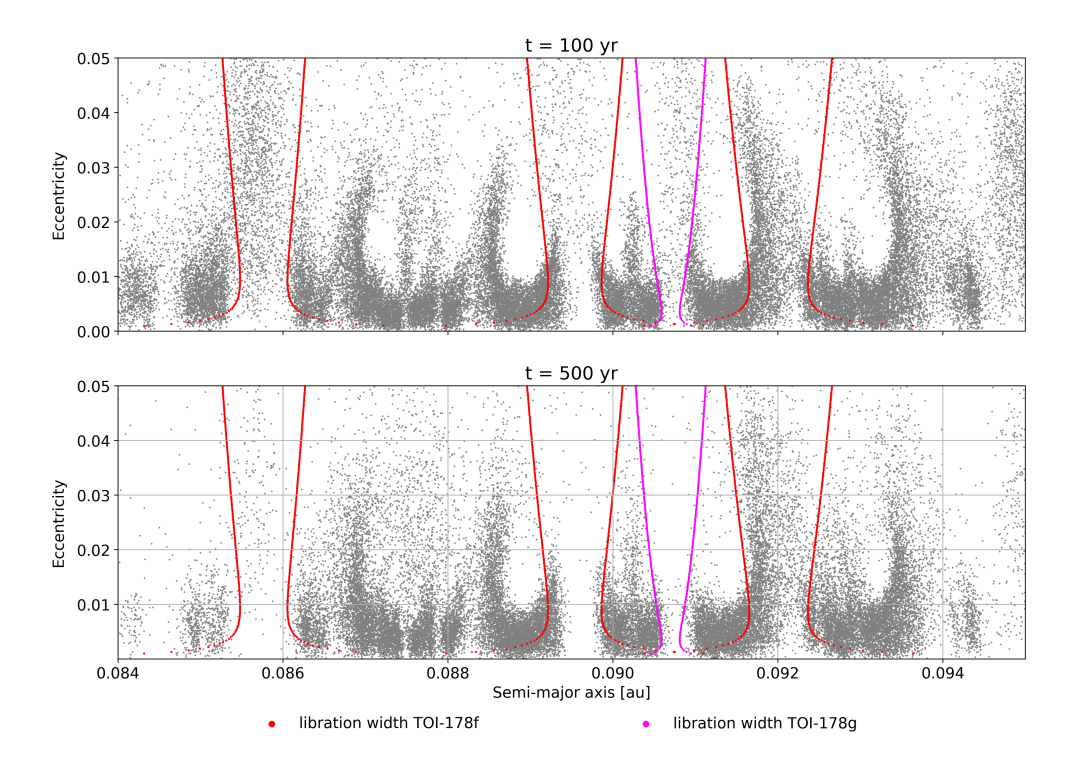


Fig. 3 Evolution of the particle distribution showing gap formation. TOI-178e (yellow) and TOI-178f (red) positions and the resonances 4:3, 5:4, 6:5 (TOI-178f) and 5:3 (TOI-178g) are indicated. The size of one bin is  $10^{-4}$  au. The inset on the top right shows the initial distribution in the same boundaries.

The structure formation in this system appears to be a natural consequence of resonant interactions between particles and the multiple planets, though whether the resonant chain configuration enhances or modifies these clearing processes compared to non-resonant multi-planet systems remains to be established through comparative studies.

The width and depth of each gap correlate with the strength of the corresponding resonance, which depends on the mass of the perturbing planet and the order of the resonance. The overlapping influence of multiple resonant planets creates gap patterns with enhanced complexity compared to single dominant perturbers, though the individual resonances remain well-described by classical theory. The libration width equation accurately predicts the locations and extents of these depleted regions, providing a theoretical framework for the observed clearing mechanisms and validating resonance theory in this multi-planet context. While classical resonance theory accurately predicts individual gap locations and widths, the simultaneous presence of multiple overlapping resonances from different planets creates a more complex clearing pattern than would be expected from the simple superposition of single-planet effects.

These results establish baseline dynamical signatures for TOI-178's unique resonant architecture, filling a significant gap in the particle dynamics literature for this



**Fig. 4** Particle depletion within libration widths. Red regions: TOI-178f resonances; magenta region: TOI-178g 5:3 resonance. The comparison between the distribution of particles after 100 yr to 500 yr shows rapid zone clearing.

system. While extensive studies exist for TRAPPIST-1's resonant chain [32, 33], TOI-178's mathematical 2:4:6:9:12 sequence had remained unexplored from a small body dynamics perspective.

# 3.4 Inner disk inclination dynamics

To investigate inclination evolution in the innermost region, we conducted an extended simulation with 10,000 test particles between 0.015-0.025 au, initialized at TOI-178c's inclination ( $88.4^{\circ}$ ). The integration spanned  $10^4$  y to capture long-term secular behavior, with outputs recorded at 2000-yr intervals.

The observed inclination oscillations arise from the natural secular evolution expected when test particles and TOI-178b are out of dynamical equilibrium [30].

Figure 5 shows the emergence of periodic inclination oscillations throughout the innermost disk region. At the beginning of the simulation (T=0), all particles maintain their initial inclination of 88.4°. By T=2000 yr, particles near 0.02 au begin to display inclination excitation, with values ranging from approximately 82° to 94°. This pattern evolves further by T=4000 yr, with the amplitude of oscillations growing noticeably.

The oscillation pattern exhibits a clear spatial structure. Particles with semi-major axes less than  $\sim 0.018$  au remain largely unaffected, maintaining inclinations close to

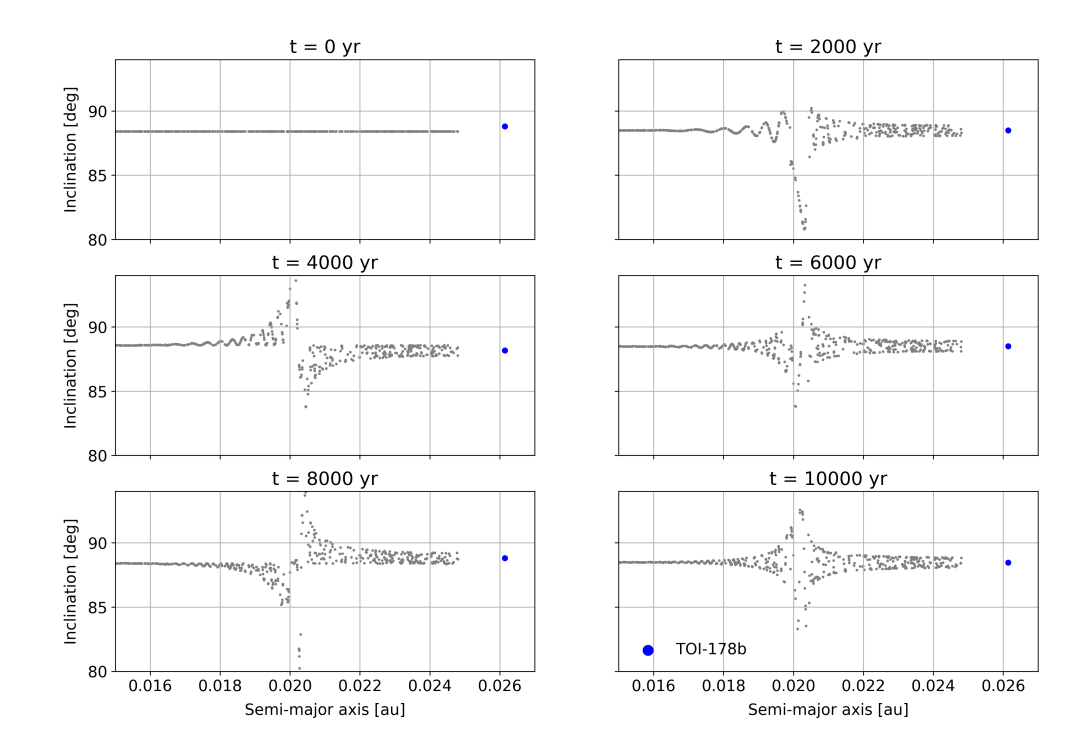


Fig. 5 Evolution of inclination showing forced oscillations. Particles are plotted in grey for six different simulation times in steps of 2000 yr and planet TOI-178b is indicated in blue.

their initial values. Between 0.018 au and 0.022 au, significant inclination variations develop, with the strongest oscillations centered at approximately 0.02 au. This spatial concentration of maximum amplitude near 0.02 au is noteworthy given that the 3:2 mean motion resonance with TOI-178b occurs at 0.01986 au, suggesting potential resonant enhancement of the secular forcing mechanism.

The pattern cycles through different configurations with a period of  $P_{\text{inc},b} = 196.078 \,\text{yr}$ , which matches TOI-178b's own inclination oscillation period. Fourier analysis of the time series confirms TOI-178b as the primary forcing agent, with the power spectrum showing a dominant peak at the frequency corresponding to  $P_{\text{inc},b}$ . While secular forcing from TOI-178b naturally explains the periodic behavior, the spatial concentration of maximum oscillation amplitude near the 3:2 resonance location suggests that mean-motion resonance proximity may amplify the secular response, though this hypothesis requires further investigation with extended simulations.

The T=6000 yr, T=8000 yr, and T=10000 yr panels demonstrate the continued stability of this oscillation pattern, with particles maintaining similar inclination distributions throughout the remainder of the simulation. The persistence of these oscillations for the full  $10^4$  years, without significant damping, indicates that they represent a stable dynamical feature of the inner TOI-178 system.

This coherent inclination behavior appears unique to the innermost region, where TOI-178b acts as the sole significant perturber. Unlike the outer regions where multiple

planets create complex, overlapping gravitational influences, the inner disk exhibits an organized, wavelike pattern characteristic of single-perturber systems. The sharp boundary of the oscillation zone at approximately 0.022 au may represent the limit of TOI-178b's dynamical influence before other planets begin to dominate the secular evolution.

# 4 Final Remarks

Our simulations of particle dynamics in the TOI-178 system suggest that its multiresonant planetary configuration influences the structure of circumstellar debris. The five outer planets in the 2:4:6:9:12 resonance chain create a dynamical environment that shapes particle distributions in ways that warrant further investigation.

The co-orbital regions appear wider than theoretical predictions, with planets in the resonance chain showing about 30% larger zones compared to Dermott and Murray [28] models. TOI-178b, which remains outside the chain, shows an even greater difference (52%). While the systematic difference between chain and non-chain planets suggests that resonant architecture may influence co-orbital dynamics, establishing direct causal relationships requires future controlled simulations with varied resonant configurations.

Between TOI-178e and TOI-178f, we identified structures resembling Kirkwood gaps, providing evidence for resonance-driven clearing mechanisms. Our analysis shows that several mean-motion resonances, particularly the 5:4 with TOI-178f and 5:3 with TOI-178g, gradually clear particles from their libration zones, similar to processes seen in our Solar System's asteroid belt.

The inclination oscillations near TOI-178b reveal an interesting dynamical phenomenon. These oscillations, mainly found between 0.018-0.022 au with maximum amplitude near the 3:2 resonance location, show how a single planet can create organized behavior in the inner disk region. The boundary at approximately 0.022 au may indicate where the influence of different planets begins to overlap.

This baseline characterization of TOI-178's architecture provides a useful case study for resonant dynamics in exoplanetary systems. The mechanisms we observed – enhanced co-orbital regions, resonance-driven gaps, and localized inclination patterns – could help explain similar features in other multi-planet systems. Future comparative studies contrasting resonant versus non-resonant planetary configurations will quantify the enhancement effects suggested by this investigation.

Acknowledgements. We thank the anonymous reviewers for their constructive comments and suggestions that significantly improved the quality of this manuscript. R.S. and C.M.S. acknowledge support by the DFG German Research Foundation (project 446102036). The authors acknowledge support by the High Performance and Cloud Computing Group at the Zentrum für Datenverarbeitung of the University of Tübingen, the state of Baden-Württemberg through bwHPC and the DFG through grant no INST 37/935-1 FUGG. R. S. also thanks CNPq (307400/2025-5).

# **Declarations**

The data supporting the findings of this study, including simulation outputs and initial conditions, are available from the corresponding author upon reasonable request.

### References

- [1] Mills, S.M., Fabrycky, D.C., Migaszewski, C., Ford, E.B., Petigura, E., Isaacson, H.: A resonant chain of four transiting, sub-Neptune planets. Nature **533**(7604), 509–512 (2016) https://doi.org/10.1038/nature17445
- [2] Izidoro, A., Ogihara, M., Raymond, S.N., Morbidelli, A., Pierens, A., Bitsch, B., Cossou, C., Hersant, F.: Breaking the chains: hot super-Earth systems from migration and disruption of compact resonant chains. Monthly Notices of the Royal Astronomical Society 470(2), 1750–1770 (2017) https://doi.org/10.1093/mnras/stx1232
- [3] Fabrycky, D.C., Lissauer, J.J., Ragozzine, D., Rowe, J.F., Steffen, J.H., Agol, E., Barclay, T., Batalha, N., Borucki, W., Ciardi, D.R., Ford, E.B., Gautier, T.N., Geary, J.C., Holman, M.J., Jenkins, J.M., Li, J., Morehead, R.C., Morris, R.L., Shporer, A., Smith, J.C., Still, M., Van Cleve, J.: Architecture of Kepler's Multitransiting Systems. II. New Investigations with Twice as Many Candidates. ApJ 790, 146 (2014) https://doi.org/10.1088/0004-637X/790/2/146
- [4] Lissauer, J.J., Fabrycky, D.C., Ford, E.B., Borucki, W.J., Fressin, F., Marcy, G.W., Orosz, J.A., Rowe, J.F., Torres, G., Welsh, W.F., Batalha, N.M., Bryson, S.T., Buchhave, L.A., Caldwell, D.A., Carter, J.A., Charbonneau, D., Christiansen, J.L., Cochran, W.D., Desert, J.-M., Dunham, E.W., Fanelli, M.N., Fortney, J.J., Gautier, T.N., Geary, J.C., Gilliland, R.L., Haas, M.R., Hall, J.R., Holman, M.J., Koch, D.G., Latham, D.W., Lopez, E., McCauliff, S., Miller, N., Morehead, R.C., Quintana, E.V., Ragozzine, D., Sasselov, D., Short, D.R., Steffen, J.H.: A closely packed system of low-mass, low-density planets transiting Kepler-11. Nature 470, 53-58 (2011) https://doi.org/10.1038/nature09760
- [5] Leleu, A., Alibert, Y., Hara, N. C., Hooton, M. J., Wilson, T. G., Robutel, P., Delisle, J.-B., Laskar, J., Hoyer, S., Lovis, C., Bryant, E. M., Ducrot, E., Cabrera, J., Delrez, L., Acton, J. S., Adibekyan, V., Allart, R., Allende Prieto, C., Alonso, R., Alves, D., Anderson, D. R., Angerhausen, D., Anglada Escudé, G., Asquier, J., Barrado, D., Barros, S. C. C., Baumjohann, W., Bayliss, D., Beck, M., Beck, T., Bekkelien, A., Benz, W., Billot, N., Bonfanti, A., Bonfils, X., Bouchy, F., Bourrier, V., Boué, G., Brandeker, A., Broeg, C., Buder, M., Burdanov, A., Burleigh, M. R., Bárczy, T., Cameron, A. C., Chamberlain, S., Charnoz, S., Cooke, B. F., Corral Van Damme, C., Correia, A. C. M., Cristiani, S., Damasso, M., Davies, M. B., Deleuil, M., Demangeon, O. D. S., Demory, B.-O., Di Marcantonio, P., Di Persio, G., Dumusque, X., Ehrenreich, D., Erikson, A., Figueira, P., Fortier,

- A., Fossati, L., Fridlund, M., Futyan, D., Gandolfi, D., García Muñoz, A., Garcia, L. J., Gill, S., Gillen, E., Gillon, M., Goad, M. R., González Hernández, J. I., Guedel, M., Günther, M. N., Haldemann, J., Henderson, B., Heng, K., Hogan, A. E., Isaak, K., Jehin, E., Jenkins, J. S., Jordán, A., Kiss, L., Kristiansen, M. H., Lam, K., Lavie, B., Lecavelier des Etangs, A., Lendl, M., Lillo-Box, J., Lo Curto, G., Magrin, D., Martins, C. J. A. P., Maxted, P. F. L., McCormac, J., Mehner, A., Micela, G., Molaro, P., Moyano, M., Murray, C. A., Nascimbeni, V., Nunes, N. J., Olofsson, G., Osborn, H. P., Oshagh, M., Ottensamer, R., Pagano, I., Pallé, E., Pedersen, P. P., Pepe, F. A., Persson, C. M., Peter, G., Piotto, G., Polenta, G., Pollacco, D., Poretti, E., Pozuelos, F. J., Queloz, D., Ragazzoni, R., Rando, N., Ratti, F., Rauer, H., Raynard, L., Rebolo, R., Reimers, C., Ribas, I., Santos, N. C., Scandariato, G., Schneider, J., Sebastian, D., Sestovic, M., Simon, A. E., Smith, A. M. S., Sousa, S. G., Sozzetti, A., Steller, M., Suárez Mascareño, A., Szabó, Gy. M., Ségransan, D., Thomas, N., Thompson, S., Tilbrook, R. H., Triaud, A., Turner, O., Udry, S., Van Grootel, V., Venus, H., Verrecchia, F., Vines, J. I., Walton, N. A., West, R. G., Wheatley, P. J., Wolter, D., Zapatero Osorio, M. R.: Six transiting planets and a chain of laplace resonances in https://doi.org/10.1051/0004-6361/202039767
- [6] Pu, B., Wu, Y.: Spacing of Kepler Planets: Sculpting by Dynamical Instability. ApJ 807, 44 (2015) https://doi.org/10.1088/0004-637X/807/1/44
- [7] Terquem, C., Papaloizou, J.C.B.: Migration and the Formation of Systems of Hot Super-Earths and Neptunes. ApJ 654, 1110-1120 (2007) https://doi.org/10. 1086/509497
- [8] Wang, J., Fischer, D.A., Horch, E.P., Huang, X.: On the Occurrence Rate of Hot Jupiters in Different Stellar Environments. AJ 154, 236 (2017) https://doi.org/ 10.3847/1538-3881/aa9216
- [9] Gillon, M., Triaud, A.H.M.J., Demory, B.-O., Jehin, E., Agol, E., Deck, K.M., Lederer, S.M., de Wit, J., Burdanov, A., Ingalls, J.G., Bolmont, E., Leconte, J., Raymond, S.N., Selsis, F., Turbet, M., Barkaoui, K., Burgasser, A., Burleigh, M.R., Carey, S.J., Chaushev, A., Copperwheat, C.M., Delrez, L., Fernandes, C.S., Holdsworth, D.L., Kotze, E.J., Van Grootel, V., Almleaky, Y., Benkhaldoun, Z., Magain, P., Queloz, D.: Seven temperate terrestrial worlds around TRAPPIST-1. Nature 542, 456–460 (2017) https://doi.org/10.1038/nature21360
- [10] Luger, R., Sestovic, M., Kruse, E., Grimm, S.L., Demory, B.-O., Agol, E., Bolmont, E., Fabrycky, D., Fernandes, C.S., Van Grootel, V., Burgasser, A., Gillon, M., Ingalls, J.G., Jehin, E., Raymond, S.N., Selsis, F., Triaud, A.H.M.J., Barclay, T., Barentsen, G., Howell, S.B., Delrez, L., de Wit, J., Foreman-Mackey, D., Holdsworth, D.L., Leconte, J., Lederer, S., Turbet, M., Almleaky, Y., Benkhaldoun, Z., Magain, P., Morris, B.M., Heng, K., Queloz, D.: A seven-planet resonant chain in TRAPPIST-1. Nature 1, 0129 (2017) https://doi.org/10.1038/

#### s41550-017-0129

- [11] Gaslac Gallardo, D.M., Giuliatti Winter, S.M., Winter, O., Callegari, N., Muñoz-Gutiérrez, M.A.: Analysing the dynamics of the Kepler-90 planetary system. MNRAS 535, 3198–3210 (2024) https://doi.org/10.1093/mnras/stae2518
- [12] Lopez, T.A., Barros, S.C.C., Santerne, A., Deleuil, M., Adibekyan, V., Almenara, J.M., Armstrong, D.J., Barrado, D., Bayliss, D., Berardo, D., Boisse, I., Bonomo, A.S., Bouchy, F., Brown, D.J.A., Lillo-Box, J., Collier Cameron, A., Delrez, L., Díaz, R.F., Doyle, A., Dumusque, X., Ehrenreich, D., Faria, J.P., Figueira, P., Foxell, E., Giles, H., Gillon, M., Hébrard, G., Hojjatpanah, S., Hobson, M., Jackman, J., King, G., Kirk, J., Lam, K.W.F., Lendl, M., Ligi, R., Lovis, C., Mousis, O., Murray, C., Osborn, H.P., Pepe, F., Pollacco, D., Santos, N.C., Sousa, S.G., Udry, S., Vigan, A.: Exoplanet characterisation in the longest known resonant chain: the K2-138 system. A&A 631, 90 (2019) https://doi.org/10.1051/0004-6361/201936267
- [13] Luque, R., Osborn, H.P., Leleu, A., Pallé, E., Bonfanti, A., Barragán, O., Wilson, T.G., Broeg, C., Cameron, A.C., Lendl, M., Maxted, P.F.L., Olofsson, G., Sousa, S.G., Serrano, L.M., Adibekyan, V., Alibert, Y., Brandeker, A., Cabrera, J., Sulis, S., Van Grootel, V., Webster, H.P., Benz, W., Deline, A., Ehrenreich, D., Fortier, A., Fridlund, M., Gandolfi, D., Güdel, M., Hoyer, S., Isaak, K.G., Queloz, D., Stalport, M., Delrez, L., Hooton, M.J., Laskar, J., Ribas, I., Udry, S., Bourrier, V., Deleuil, M., Dumusque, X., Hara, N.C., Allart, R., Alonso, R., Anderson, D.R., Anglada-Escudé, G., Bárczy, T., Barrado Navascues, D., Barros, S.C.C., Baumjohann, W., Beck, M., Beck, T., Billot, N., Biondi, F., Borsato, L., Buder, M., Castro-González, A., Charnoz, S., Ciardi, D.R., Cloutier, R., Cochran, W.D., Collins, K.A., Conti, D.M., Crossfield, I.J.M., Csizmadia, S., Cubillos, P.E., Davies, M.B., Demangeon, O.D.S., Demory, B.-O., Dragomir, D., Dransfield, G., Ehrenreich, D., Erikson, A., Essack, Z., Farinato, J., Fossati, L., Gill, S., Gillon, M., Goad, M.R., Guedel, M., Günther, M.N., Haldemann, J., Henderson, B.A., Heng, K., Hooton, M.J., Isaak, K.G., Jenkins, J.M., Jenkins, J.S., Jordán, A., Kiss, L., Kristiansen, M.H., Lam, K., Lavie, B., Lecavelier des Etangs, A., Lillo-Box, J., Livingston, J.H., Magrin, D., Maxted, P.F.L., Mordasini, C., Moyano, M., Murray, C.A., Nascimbeni, V., Olofsson, G., Osborn, H.P., Ottensamer, R., Pagano, I., Peter, G., Piotto, G., Pollacco, D., Queloz, D., Ragazzoni, R., Rando, N., Rauer, H., Ribas, I., Ricker, G., Salmon, S., Santos, N.C., Scandariato, G., Seager, S., Ségransan, D., Simon, A.E., Smith, A.M.S., Steller, M., Sulis, S., Szabó, G.M., Thomas, N., Tilbrook, R.H., Triaud, A.H.M.J., Udry, S., Ulmer, B., Van Grootel, V., Vanderspek, R., Venturini, J., Walton, N.A., Winn, J.N.: A resonant sextuplet of sub-Neptunes transiting the bright star HD 110067. Nature **623**, 932–937 (2023) https://doi.org/10.1038/s41586-023-06692-3
- [14] Mustill, A.J., Villaver, E., Veras, D., Gänsicke, B.T., Bonsor, A.: Foretellings of Ragnarök: World-engulfing Asymptotic Giants and the Inheritance of White Dwarfs. MNRAS 478, 2896–2909 (2018) https://doi.org/10.1093/mnras/sty1273

- [15] Tamayo, D., Cranmer, M., Hadden, S., Rein, H., Battaglia, P., Obertas, A., Armitage, P.J., Ho, S., Spergel, D.N., Gilbertson, C., Hussain, N., Silburt, A., Jontof-Hutter, D., Menou, K.: Predicting the long-term stability of compact multiplanet systems. Proceedings of the National Academy of Science 117, 18194–18205 (2020) https://doi.org/10.1073/pnas.2001258117
- [16] Shannon, A., Dawson, R.I.: The resonance overlap and Hill stability criteria revisited. MNRAS 462, 2735–2747 (2016) https://doi.org/10.1093/mnras/stw1822
- [17] Delrez, L., Leleu, A., Brandeker, A., Gillon, M., Hooton, M.J., Cameron, A.C., Deline, A., Fortier, A., Queloz, D., Bonfanti, A., Van Grootel, V., Wilson, T.G., Egger, J.A., Alibert, Y., Alonso, R., Anglada, G., Asquier, J., Bárczy, T., Barrado y Navascues, D., Barros, S.C.C., Baumjohann, W., Beck, M., Beck, T., Benz, W., Billot, N., Bonfils, X., Borsato, L., Broeg, C., Buder, M., Cabrera, J., Cessa, V., Charnoz, S., Csizmadia, S., Cubillos, P.E., Davies, M.B., Deleuil, M., Demangeon, O.D.S., Demory, B.-O., Ehrenreich, D., Erikson, A., Fossati, L., Fridlund, M., Gandolfi, D., Güdel, M., Hasiba, J., Hover, S., Isaak, K.G., Jenkins, J.M., Kiss, L.L., Laskar, J., Latham, D.W., Lecavelier des Etangs, A., Lendl, M., Lovis, C., Luque, R., Magrin, D., Maxted, P.F.L., Mordasini, C., Nascimbeni, V., Olofsson, G., Ottensamer, R., Pagano, I., Pallé, E., Peter, G., Piotto, G., Pollacco, D., Ragazzoni, R., Rando, N., Rauer, H., Ribas, I., Ricker, G., Santos, N.C., Scandariato, G., Seager, S., Ségransan, D., Simon, A.E., Smith, A.M.S., Sousa, S.G., Steller, M., Szabó, G.M., Thomas, N., Udry, S., Vanderspek, R., Venturini, J., Viotto, V., Walton, N.A., Winn, J.N.: Refining the properties of the TOI-178 system with CHEOPS and TESS. A&A 678, 200 (2023) https://doi.org/10.1051/0004-6361/202245479
- [18] Leleu, A., Delisle, J.-B., Delrez, L., Bryant, E.M., Brandeker, A., Osborn, H.P., Hara, N., Wilson, T.G., Billot, N., Lendl, M., al.: Photo-dynamical characterisation of the TOI-178 resonant chain: Exploring the robustness of TTV and RV mass characterisation. Astronomy & Astrophysics 685, 221 (2024) https: //doi.org/10.1051/0004-6361/202347790
- [19] Quarles, B., Li, G., Rosario-Franco, M.: Application of Orbital Stability and Tidal Migration Constraints for Exomoon Candidates. ApJ **902**(1), 20 (2020) https://doi.org/10.3847/2041-8213/abba36 arXiv:2009.14723 [astro-ph.EP]
- [20] Unterborn, C.T., Desch, S.J., Hinkel, N.R., Lorenzo, A.: Inward migration of the TRAPPIST-1 planets as inferred from their water-rich compositions. Nature 2, 297–302 (2018) https://doi.org/10.1038/s41550-018-0411-6
- [21] Grimm, S.L., Demory, B.-O., Gillon, M., Dorn, C., Agol, E., Burdanov, A., Delrez, L., Sestovic, M., Triaud, A.H.M.J., Turbet, M., Bolmont, E., Caldas, A., de Wit, J., Jehin, E., Leconte, J., Raymond, S.N., Van Grootel, V., Burgasser, A.J., Carey, S., Fabrycky, D., Heng, K., Hernandez, D.M., Ingalls, J.G., Lederer, S., Selsis,

- F., Queloz, D.: The nature of the TRAPPIST-1 exoplanets. A&A **613**, 68 (2018) https://doi.org/10.1051/0004-6361/201732233
- [22] Wisdom, J.: The origin of the Kirkwood gaps: A mapping for asteroidal motion near the 3/1 commensurability. AJ 87, 577–593 (1982) https://doi.org/10.1086/113132
- [23] Morbidelli, A.: Modern Celestial Mechanics : Aspects of Solar System Dynamics, (2002)
- [24] Nesvorný, D.: Dynamical Evolution of the Early Solar System. ARA&A **53**, 45–88 (2015) https://doi.org/10.1146/annurev-astro-082214-122302
- [25] Rein, H., Liu, S.-F.: REBOUND: an open-source multi-purpose N-body code for collisional dynamics. A&A 537, 128 (2012) https://doi.org/10.1051/0004-6361/ 201118085 arXiv:1110.4876 [astro-ph.EP]
- [26] Rein, H., Spiegel, D.S.: IAS15: A fast, adaptive, high-order integrator for gravitational dynamics, accurate to machine precision over a billion orbits. Monthly Notices of the Royal Astronomical Society 446(2), 1424–1437 (2015) https://doi.org/10.1093/mnras/stu2164 arXiv:1409.4779 [astro-ph.EP]
- [27] Margot, J.L.: A Quantitative Criterion for Defining Planets. In: 47th Annual Lunar and Planetary Science Conference. Lunar and Planetary Science Conference, p. 2699 (2016)
- [28] Dermott, S.F., Murray, C.D.: The dynamics of tadpole and horseshoe orbits
   I. Theory. Icarus 48(1), 1–11 (1981) https://doi.org/10.1016/0019-1035(81) 90147-0
- [29] Kirkwood, D.: Meteoric Astronomy: a Treatise on Shooting-stars, Fireballs, and Aerolites., (1867)
- [30] Murray, C.D., Dermott, S.F.: Solar System Dynamics, (1999). https://doi.org/ 10.1017/CBO9781139174817
- [31] Nesvorný, D., Morbidelli, A.: Dynamics of small bodies in planetary systems. Annual Review of Astronomy and Astrophysics **56**, 137–174 (2018)
- [32] Garraffo, C., Drake, J.J., Cohen, O.: The space weather of proxima centauri b. The Astrophysical Journal Letters 833(1), 4 (2017)
- [33] Teyssandier, J., Libert, A.-S.: Trappist-1: Dynamical analysis of the transit-timing variations and origin of the resonant chain. Astronomy & Astrophysics **658**, 170 (2022)